Structural and electronic properties of *n*-doped and *p*-doped $SrTiO_3$

Weidong Luo,[1,2] Wenhui Duan,[1,3] Steven G. Louie,[1,2] and Marvin L. Cohen[1,2]
[1]*Department of Physics, University of California at Berkeley, Berkeley, California 94720, USA*
[2]*Materials Sciences Division, Lawrence Berkeley National Laboratory, Berkeley, California 94720, USA*
[3]*Department of Physics, Tsinghua University, Beijing 100084, China*
(Received 24 August 2004; published 17 December 2004)

We study the effects of *n*-doping and *p*-doping on the structural and electronic properties of $SrTiO_3$ using the *ab initio* pseudopotential density functional theory. Two types of electron doping and one type of hole doping are considered: introducing O vacancies, substituting V for Ti, and substituting Sc for Ti. We find that all dopings lead to small structural distortions. The effect of O vacancies on the structure is the largest. Electron doping leads to significant changes of the conduction band. For the O vacancy case, there is a Ti $3d$-e_g type defect state near the lower conduction band; while in the case of substitutional V, some parts of the lowest conduction bands become very flat. Hole doping yields a larger density of states at the Fermi level than electron doping. Our results indicate that the rigid band model with a Fermi level shift upwards or downwards is not applicable to describe the effects of oxygen vacancy induced electron doping on the electronic properties; however, this may be a reasonable approximation for the case of hole doping. Finally, we estimate the electron-phonon coupling parameters and discuss the implications of this study on superconductivity in the $SrTiO_3$ system.

DOI: 10.1103/PhysRevB.70.214109 PACS number(s): 61.72.Ww, 61.72.Ji, 71.55.Ht, 61.72.Bb

I. INTRODUCTION

Strontium titanate ($SrTiO_3$), as an incipient ferroelectric and one of the most widely used electronic ceramic materials, has attracted much attention because of its anomalous dielectric properties and considerable potential for technological application. This material remains a paraelectric down to 0 K because of quantum effects, and the tetragonal distortion below the antiferrodistortive structural phase transition at 105 K.[1] The susceptibility saturates at a large value of 20 000 as temperature approaches zero. The absence of a ferroelectric transition is suggested to be caused by quantum fluctuations, which give rise to a quantum paraelectric phase at very low temperature.[2,3]

Recently, the behavior of doped $SrTiO_3$ has been widely studied in an attempt to understand the rich variations in physical properties arising from carrier doping.[4–11] Stoichiometric $SrTiO_3$ is a band insulator with an indirect band gap of 3.25 eV.[12] Electron doping can be realized by introducing O vacancies, substituting La for Sr or substituting Nb for Ti, and other similar substitutions. It has been found that electron doping can transform insulating $SrTiO_3$ into a metallic state even with small doping levels.[4–9] When doped with substitutional Sc for Ti, $SrTiO_3$ exhibits hole conductivity as well as protonic conductivity. Photoemission spectroscopy measurements suggest that the band structure of *p*-type $SrTiO_3$ can be understood using a rigid-band model with a lower Fermi level.[10] Compared with the studies for electron doping, theoretical investigations for hole doping in $SrTiO_3$ are rare.

An interesting property of the doped $SrTiO_3$ system is superconductivity. First principles calculations for perfect $SrTiO_3$ have exhibited a flat conduction band,[13,14] which corresponds to a high density of states (DOS) and strong screening of the Coulomb interaction. This should be favorable for a superconducting transition according to the conventional BCS theory of superconductivity. Noting that $SrTiO_3$ has a high static dielectric constant, large electron effective mass, and can be highly doped, it was suggested[15] that $SrTiO_3$ could be superconducting, and this prediction was experimentally confirmed.[16–20] The superconducting transition has been observed for $SrTiO_3$ specimens with electron carrier concentration n as low as 6.9×10^{18} cm^{-3}.[17] Although the ratio T_c/n is of the same order as in cuprate superconductors, the superconducting transition temperature T_c observed in $SrTiO_{3-x}$ is lower than 1 K.

There are many interesting properties of superconducting $SrTiO_3$. For example, the measured curve of T_c versus n for $SrTiO_3$ contains a maximum value of T_c and then a decrease, which is contrary to results using the BCS model of a monotonic dependence of $\ln T_c$ on $n^{1/3}$. It is clear that a comprehensive knowledge of doping induced changes of the electronic structure is essential for understanding the normal and superconducting state properties of $SrTiO_3$ systems.

In the present work we explore the dependence of the structural and electronic properties of $SrTiO_3$ on electron and hole doping, and attempt to clarify the implications of doping on the superconductivity. First principles calculations within density functional theory are conducted to demonstrate the effects of doping on the atomic structure and energy bands. The electron-phonon coupling strength is also estimated. This paper is organized as follows. Section II gives a brief description of the model and the method used in the calculations. The calculated results are presented in Sec. III with analyses. A summary is presented in Sec. IV.

II. MODEL AND METHOD

At room temperature, undoped $SrTiO_3$ has an ideal cubic $Pm3m$ perovskite structure with Ti atoms at the cube center,

TABLE I. Calculated and experimental structural parameters and band gaps of undoped $SrTiO_3$.

	Lattice constant (a.u.)	Bulk modulus (GPa)	Indirect gap ($R_v \rightarrow \Gamma_c$) (eV)	Direct gap (at Γ) (eV)
Expt.	7.38[a]	183[a]	3.25[b]	3.75[b]
This work	7.368	200	2.04	2.28
PP method[c]	7.303	199		
OLCAO method[d]	7.429	163	1.45	1.98
FPLAPW method[e]	7.30	203	1.84	

[a]Reference 30.
[b]Reference 12.
[c]Reference 13.
[d]Reference 14.
[e]Reference 31.

Sr atoms at the cube corner and O atoms at the face centers. The cubic unit cell contains one molecule of $SrTiO_3$. Most of the simulations for *n* and *p* dopings are performed using a 40 atom supercell, containing eight $SrTiO_3$ unit cells ($2\times2\times2$). For the case of oxygen vacancy doping, an 80 atom supercell ($2\times2\times4$) is also used (the supercell is doubled along the Ti-Vac-Ti direction). Doping is generated in the supercell by removing a single O atom, substituting a V atom for a Ti atom, or substituting a Sc atom for a Ti atom. Correspondingly, the compositions are $SrTiO_{2.875}$, $Sr(Ti_{2.875}V_{0.125})O_3$, $Sr(Ti_{2.875}Sc_{0.125})O_3$ for the 40 atom supercell, and $SrTiO_{2.9375}$ for the 80 atom supercell.

Our calculations employ pseudopotentials and the density functional theory[21,22] within the local density approximation (LDA).[23] A detailed description of the method can be found elsewhere.[24,25] We use the norm-conserving Troullier-Martins pseudopotentials[26] with partial core corrections.[27] In each doping case, both the lattice parameters and the internal atomic coordinates are relaxed to minimize the total energy.[28] We choose a plane-wave energy cutoff of 100 Ry, with a *k*-grid of $2\times2\times2$ points in the full Brillouin zone for the supercell calculations (a $4\times4\times4$ *k*-grid is used for the undoped $SrTiO_3$ calculation, and a $2\times2\times1$ *k*-grid for the $2\times2\times4$ supercell).

III. RESULTS AND DISCUSSIONS

Table I lists the calculated and experimental lattice constant, bulk modulus, and band gaps of undoped $SrTiO_3$ in the cubic phase. The calculated lattice constant and bulk modulus are in good agreement with experimental measurements and with other theoretical results. Note that in the pseudopotential calculation of Ref. 13, the semicore states of Sr and Ti are treated as valence states when constructing the pseudopotentials. Our calculated band gaps are less than experimental values, which is typical for LDA calculations. Figure 1 shows the band structure and density of states for undoped $SrTiO_3$, respectively. The results depict $SrTiO_3$ as an indirect insulator with the top of the valence band at *R* and the bottom of the conduction band at Γ. The lowest conduction band from Γ to *X* is quite flat, which was found to be a common feature of many ABO_3 perovskite ferro-

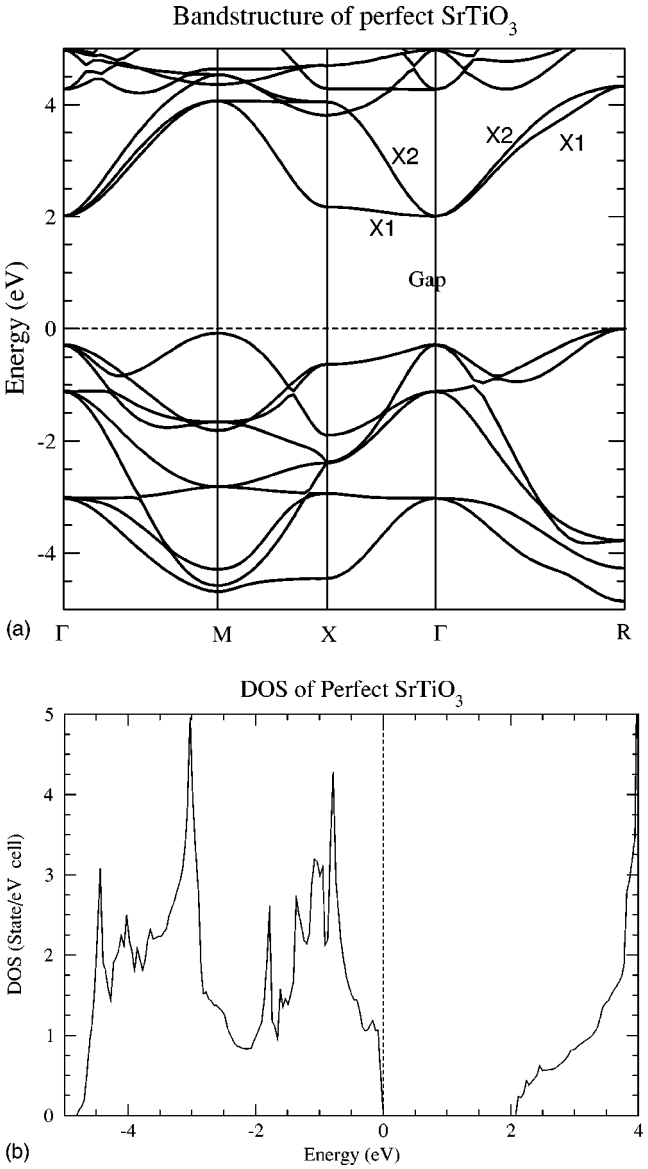

FIG. 1. Undoped $SrTiO_3$: (a) Energy band structure and (b) density of states. The zero of energy is set at the top of the valence band.

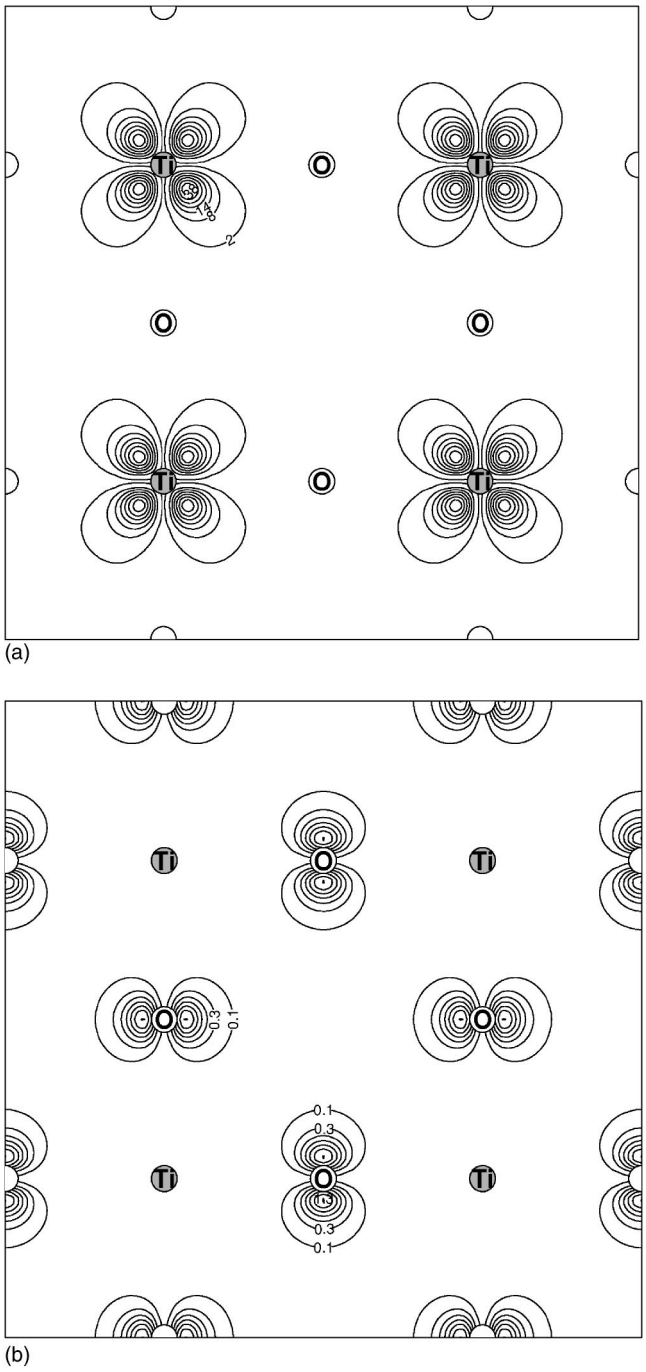

FIG. 2. (a) $|\Psi_\Gamma|^2$ of the lowest conduction band (Ti $3d$-t_{2g} orbitals) and (b) $|\Psi_R|^2$ of the highest valence band (O $2p$ orbitals) in the Ti-O plane for undoped $SrTiO_3$. Here Ψ_Γ and Ψ_R are wave functions at Γ and R.

electrics.[13,29] It is well known that the electronic properties of the doped systems can sensitively depend on the electronic structure near the top of valence band and near the bottom of the conduction band. Figure 2 shows $|\Psi_R|^2$ and $|\Psi_\Gamma|^2$ throughout the Ti-O plane, respectively. Here Ψ_R and Ψ_Γ are electron wave functions at R point of the highest valence band and at Γ point of the lowest conduction band, respectively. It is clear that Ψ_R is predominantly composed of O $2p$ orbitals and Ψ_Γ is predominantly composed of Ti $3d$-t_{2g} orbitals. In fact, because of the cubic crystal field produced by the six nearest-neighbor O atoms, the empty Ti $3d$ orbitals will split into three lower energy t_{2g} orbitals (xy,yz,zx) and two higher energy e_g orbitals $(3z^2-r^2, x^2-y^2)$. This can be clearly seen by the threefold degenerate states at the conduction band minimum and the twofold degenerate states which are 2.3 eV higher in energy (at Γ).

Now we examine the effect of O vacancy doping on the structural and electronic properties. For undoped $SrTiO_3$, our calculated Sr-O and Ti-O distances are 2.757 Å and 1.950 Å, respectively. We find that introducing O vacancies leads to a slight distortion from the cubic phase to the tetragonal phase. For the 40 atom supercell, the vacancy-induced changes of the bond lengths are less than 0.06 Å for the Sr-O bond and 0.04 Å for the Ti-O bond. We observe that the nearest four Sr^{2+} cations of an O vacancy are displaced away from the vacancy, while the nearest two Ti^{4+} cations and eight O^{2-} anions move toward the vacancy. For the 80 atom supercell, the relaxation of the atomic positions is slightly larger and different. The two nearest Ti^{4+} cations move away from the vacancy by 0.05 Å while the distances between these two Ti atoms and their nearest-neighbor O atoms along the Ti-Vac-Ti direction decrease by 0.086 Å. This is in agreement with the previous work on charged O vacancies in $SrTiO_3$ by Astala and Bristowe[8,32] which showed small atomic relaxations with O vacancies.

We are most interested in the doping-induced change of the band structure around the Fermi level. Figure 3 shows the band structure and DOS of $SrTiO_{2.875}$. For this case, the Fermi level is in the conduction band and the DOS at the Fermi level is no longer zero because of the carriers arising from O vacancies. Hence the doped system is metallic. Based only on a comparison of the DOS, i.e., Figs. 1(b) and 3(b), a rigid band model appears to be proper for describing the effect of electron doping on electronic properties, as suggested by Shanthi and Sarma.[5] However, Fig. 3(a) reveals a different picture since the vacancy-induced change of the conduction band is significant. In other words, some of the conduction bands are not rigid when introducing O vacancies. Since a $2\times2\times2$ supercell is used in our calculations for doped $SrTiO_3$, it is instructive to consider the band folding effects while comparing the band structure of Fig. 3(a) with that of undoped $SrTiO_3$ [shown in Fig. 1(a)]. The band structure of undoped $SrTiO_3$ with a $2\times2\times2$ supercell can be obtained directly from the band structure plotted in the conventional unit cell [shown in Fig. 1(a)] by band folding. For example, three equivalent X points of the Brillouin zone of the conventional unit cell fold into the zone center (Γ point). From Fig. 1(a), we can see that the lowest level at X of the conduction bands is nondegenerate. For undoped $SrTiO_3$ in a $2\times2\times2$ supercell, there would be six low lying Γ levels, three are associated with the original degenerate Γ states and the other three arise from folded X states. These six states are much lower in energy than other levels in the conduction bands, and therefore have a large influence on the electronic properties. It is interesting to note that when there is one O vacancy in the $2\times2\times2$ supercell, there are seven Γ levels near the Fermi level in the conduction bands, as shown in Fig. 3(a). One of the lowest conduction bands originate from the O vacancy. In order to clarify this point, we analyze

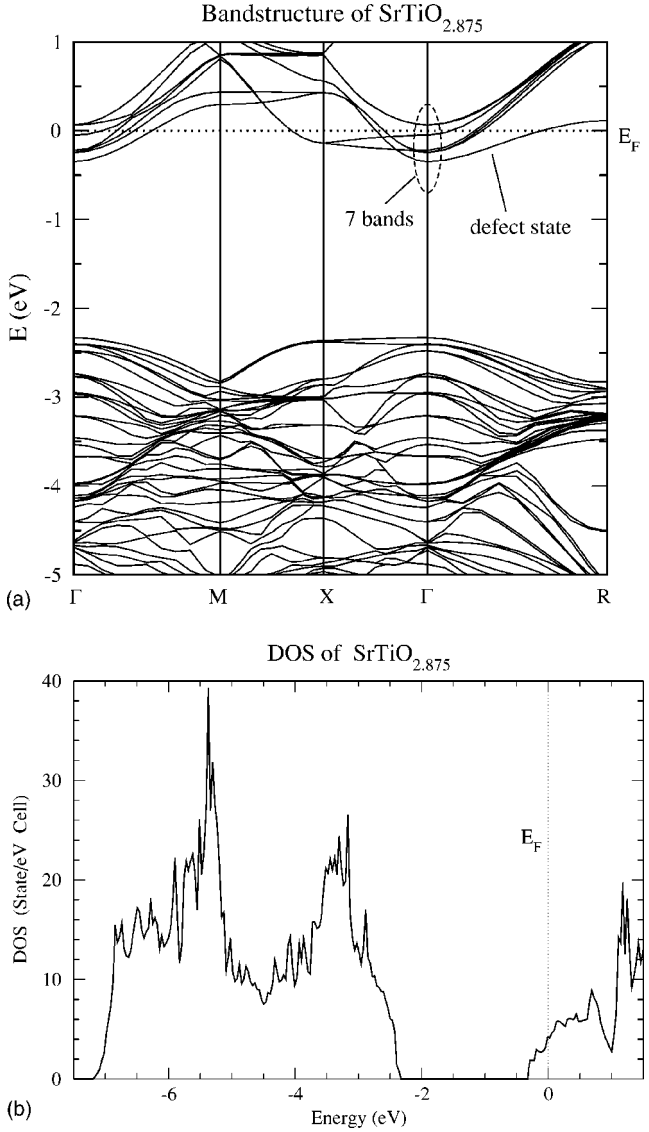

FIG. 3. (a) Energy band structure and (b) the density of states (DOS) of $SrTiO_{2.875}$. The zero of energy is set at the Fermi energy. Note that a $2\times2\times2$ supercell is used, so the volume of the cell is eight times as large as in the case of the undoped calculation.

$|\Psi_\Gamma|^2$ for all seven lowest conduction bands where Ψ_Γ is the the wave function at Γ. We find that, in the lowest conduction band, mostly the e_g type orbitals ($3z^2-r^2$, with z axis along the Ti-Vac-Ti direction) of the two nearest Ti atoms to the vacancy contribute to $|\Psi_\Gamma|^2$, and other atoms have only small contributions to $|\Psi_\Gamma|^2$ as shown in Fig. 4(a). The $|\Psi_\Gamma|^2$ for the other six lowest conduction bands are predominantly composed of Ti $3d$-t_{2g} orbitals, as shown in Fig. 4(b). For these six bands, all Ti atoms (no matter whether they are close to the vacancy or not) have similar contributions to $|\Psi_\Gamma|^2$, which is also very similar to the picture shown in Fig. 2(a) for undoped $SrTiO_3$. Therefore we may conclude that the lowest conduction band originates from a Ti $3d$-e_g type defect state, and the other six conduction bands are associated with the band folding states of the three lower conduction bands (mainly Ti $3d$-t_{2g} orbitals) of the undoped $SrTiO_3$. This again indicates that the effect of electron doping by introducing O vacancies cannot be correctly analyzed within a rigid band model.

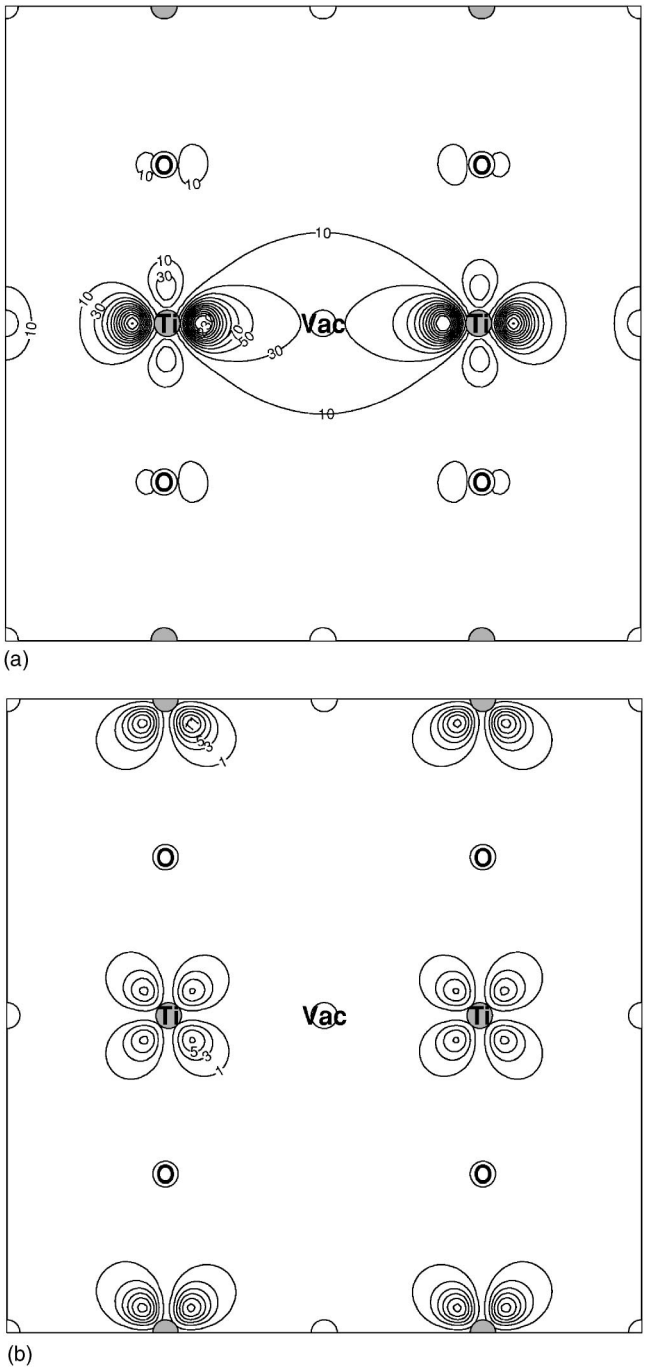

FIG. 4. (a) $|\Psi_\Gamma|^2$ of the oxygen vacancy induced defect state (mainly Ti $3d$-e_g type states) and (b) the lowest conduction band (Ti $3d$-t_{2g} state) above the defect state of $SrTiO_{2.875}$ in the Ti-O plane. Here Ψ_Γ is the wave function at Γ.

We note that in the 40 atom supercell calculations, the Ti $3d$-e_g type defect states have lower energy than the Ti $3d$-t_{2g} type conduction states. This is actually easy to understand, considering that the $3z^2-r^2$ type orbital concentrates its charge density in a direction toward two of the nearest O atoms, while one of them (the one in the vacancy site) is missing and the Ti atom moves away from the other O atom

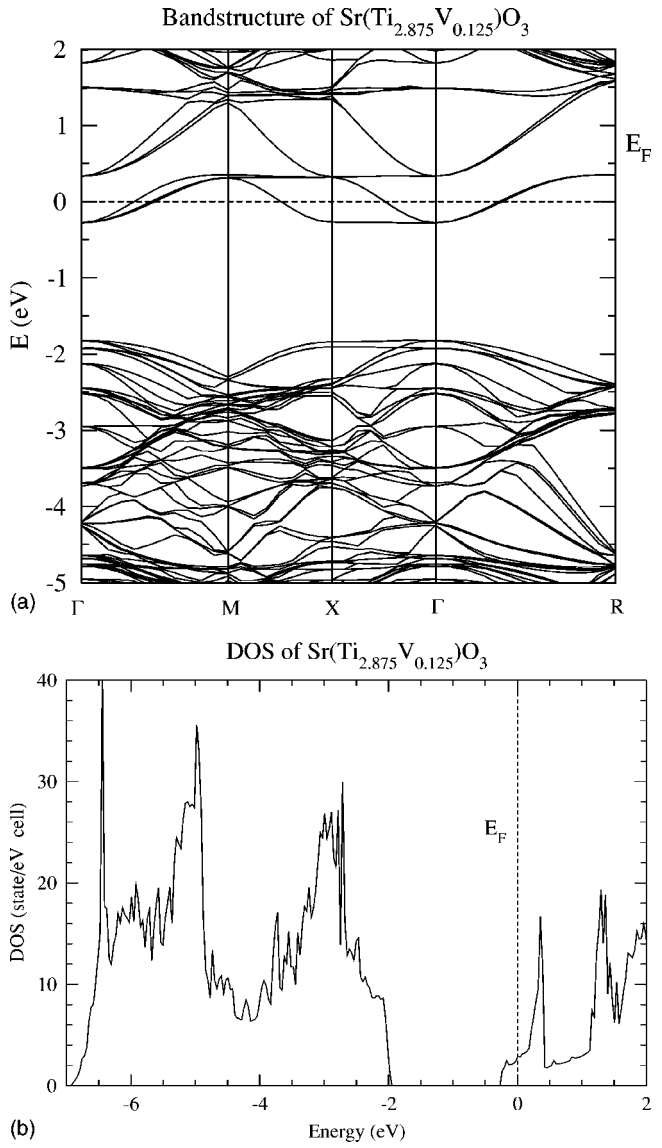

FIG. 5. (a) Energy band structure and (b) the density of states (DOS) of $Sr(Ti_{2.875}V_{0.125})O_3$. The zero of energy is set at the Fermi energy. The supercell volume is used when calculating the DOS.

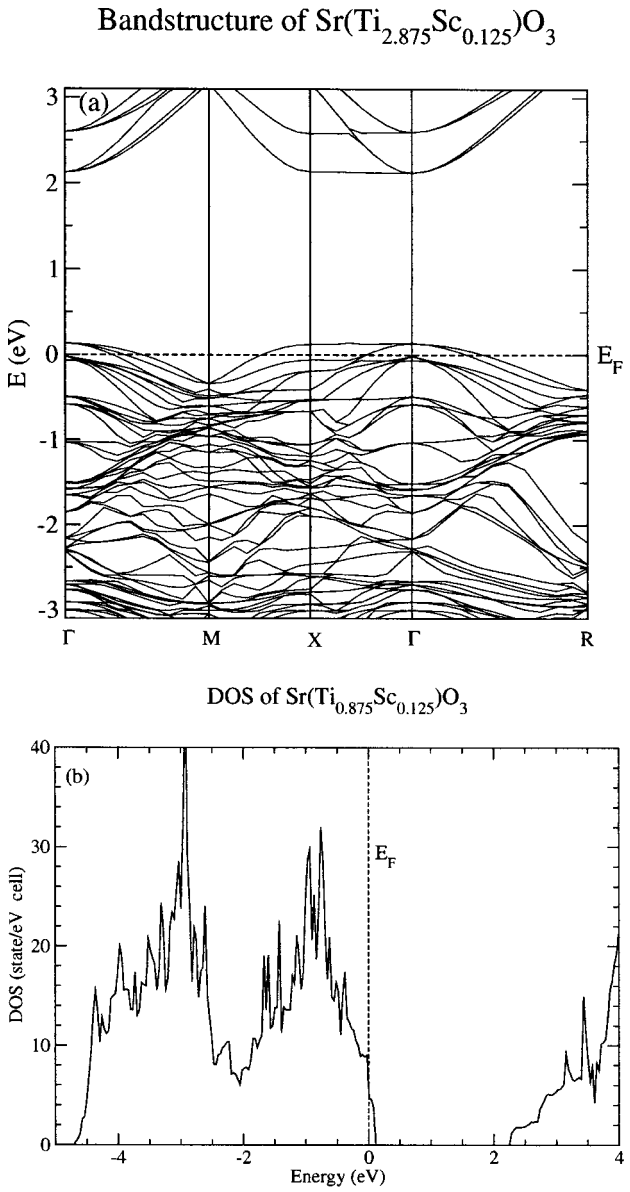

FIG. 6. (a) Energy band structure and (b) the density of states (DOS) of $Sr(Ti_{2.875}Sc_{0.125})O_3$. The zero of energy is set at the Fermi energy. Again the supercell volume is used when calculating the DOS.

by about 0.034 Å. From the energy dispersion of the defect state [Fig. 3(a)] and the spatial extension of the defect wave function [Fig. 4(a)], there is considerable interaction of the defect wave functions along the Ti-Vac-Ti direction between neighboring supercells. To address this problem, we repeat the calculations with a doubled supercell (80 atoms). Compared to the 40 atom supercell, there are two important differences in the electronic band structure. First, the defect band dispersion becomes almost flat with a bandwidth of 0.3 eV, which is the result of reduced interaction between defect wave functions due to a larger supercell. Second, for the two Ti atoms next to the O vacancy, the distance to their other nearest-neighboring O atoms along the Ti-Vac-Ti is reduced by 0.086 Å compared to the undoped structure. The enhanced crystal field caused by the closer O atoms lifts up the e_g type defect states. This shifts its energy level to 0.40 eV higher than the conduction band minimum and above the Fermi level. Thus the defect state becomes completely empty.

In a recent publication,[33] Ricci *et al.* observed a similar impurity state in the band gap associated with the oxygen vacancy, although they did not see the shifting of the impurity energy due to lack of relaxation of the internal atomic coordinates. In another recent paper on the oxygen vacancy by Buban *et al.*,[34] it is claimed that the defect wave function changes its character from a deep to a shallow level by going from a 40 atom supercell to a 160 atom (and 320 atom) supercell. While the defect wave function in their 40 atom supercell calculation is similar to the Ti $3d$-e_g type defect state wave function in our calculation, the shallow-level-like defect state in their 160 atom (and 320 atom) supercell calculations is strikingly similar to the conduction state above

the defect state in our calculation [see Fig. 4(b)]. It is possible that the shallow-level-like defect state they had is actually one of the Ti $3d$-t_{2g} type (xy,yz,zx) conduction bands, while the real e_g type defect state is higher in energy and is unoccupied as shown in the present study using 80 atom supercells. Since the defect state energy sensitively depends on the distance between neighboring vacancy sites and the neighboring oxygen environment of the Ti atoms closest to the vacancy, we expect the clustering of oxygen vacancies[5] could lower the defect state energy. This could trap doped electrons in localized states which could give an explanation of the discrepancy between the density of doped electrons determined using Hall effect data and by oxygen vacancy density.[35] A recent experimental study on $SrTiO_3$ superlattice films suggests that oxygen vacancy clustering occurs in $SrTiO_3$ films and the oxygen doping profile can change drastically within a few atomic layers.[36] We can expect that clusters of oxygen vacancies in $SrTiO_3$ become energetically favored compared to isolated vacancies. It is possible that clusters of oxygen vacancies will have much smaller diffusion coefficients than that of a single isolated vacancy, thus providing a mechanism for the nanometer-scale abruptness of oxygen doping profile, which has great implication for the growth of high quality thin film nanostructure in $SrTiO_3$.

It is expected that doping *n*-type with substitution of V for Ti has less effect on the atomic structure of the system than by introducing O vacancies. Our calculation shows that structural relaxation due to substitutional V is quite small. The six nearest O anions of the V^{5+} cation are displaced toward the substitutional V. The calculated bond length of the V-O bond is 1.920 Å which is slightly less than the Ti-O bond length (1.950 Å) in undoped $SrTiO_3$. This is in agreement with the fact that the ionic radius of the V^{5+} ion is less than that of the Ti^{4+} ion. Figure 5 shows the band structure and DOS of $Sr(Ti_{2.875}V_{0.125})O_3$, respectively. We can clearly see that due to substitutional V, the Fermi energy shifts into the conduction bands and the system is metallic. There are six conduction bands around the Fermi level, and these six conduction bands are split in energy into two groups, with three bands in each group. The three lower energy bands join with the three higher energy bands at the X points. The splitting is likely due to the difference of potential energies between V^{5+} and Ti^{4+} ions. The three lowest conduction bands are partially occupied and the other three conduction bands with higher energy are unoccupied. Within the three partially occupied conduction bands, both the band minimum from Γ to X and the band maximum from X to R are very flat. Because of the phase space factor, only the band maximum produces a large density of states at the energy about 0.4 eV above the Fermi level and the DOS at the Fermi level is only 2.80 states/eV cell.

The above results indicate that O vacancy doping and V substitution of Ti can lead to significant changes for the conduction bands. Although some conduction bands are rather flat when doping *n*-type, in general, the density of states at the Fermi level is not enhanced significantly. Hence, increasing the density of doping electrons might not be useful for significantly increasing T_c of doped $SrTiO_3$ systems.

It is interesting to explore the case of hole doping. From Fig. 2(b), we see that the highest valence band is predominantly composed of O $2p$ orbitals. It is reasonable to expect that hole doping achieved by substituting Sc for Ti should not significantly affect the top of the valence bands. Our calculations show that the highest valence band from R to M, which is not shown in Fig. 1(a), is very flat with an energy difference of less than 0.07 eV for undoped $SrTiO_3$. This means that the holes at the top of the valence band may have larger effective masses and the DOS at the Fermi level could be higher than for *n*-type systems. Therefore it would be interesting to explore whether hole doping provides an alternate way to improve the T_c of doped $SrTiO_3$ systems. In the present work, we study the hole doping realized by substituting Sc for Ti, as described in Sec. II. Our calculations show that for $Sr(Ti_{2.875}Sc_{0.125})O_3$, the structural relaxation due to hole doping is small, similar to the case of substitutional electron doping. The six nearest O anions of Sc^{3+} cation are displaced away from the substitutional Sc. The calculated bond length of the Sc-O bond is 2.005 Å which is slightly larger than the Ti-O bond length (1.950 Å) in undoped $SrTiO_3$. This is consistent with the fact that the ionic radius of Sc is larger than that of Ti. Figure 6 shows the band structure and DOS of $Sr(Ti_{2.875}Sc_{0.125})O_3$. We can see that the Fermi energy shifts downwards into the original valence bands due to substitutional Sc, and the system becomes metallic. Although there is a remarkable change of the lower conduction bands [as shown in Fig. 6(a)], the band structure around the Fermi level is not significantly affected by the hole doping and is similar to the top valence band structure of undoped $SrTiO_3$ (note, band-folding effects should be included when making this comparison). This, as well as the similarity between Fig. 1(b) and Fig. 6(b), indicates that the rigid band model is roughly valid for $SrTiO_3$ with hole doping when the doping concentration is not very high. The calculated DOS at the Fermi level is about 4.62 states/eV cell, which is larger than that of $SrTiO_{2.875}$ (4.18 states/eV cell) and that of $Sr(Ti_{2.875}V_{0.125})O_3$ (2.80 states/eV cell). Note that the doped electron density in $SrTiO_{2.875}$ is twice the doped electron density in $Sr(Ti_{2.875}V_{0.125})O_3$ and the doped hole density in $Sr(Ti_{2.875}Sc_{0.125})O_3$. It seems that hole doping can provide a higher DOS at the Fermi level than electron doping for the same carrier density. Fig. 6(b) also shows that the DOS at the Fermi level may increase sharply by slightly increasing the hole doping density.

In order to compare the possible superconducting transition properties of the electron and hole doped $SrTiO_3$ systems, we also estimate the electron-phonon coupling strength. We study the perfect system without doping, which should be a good approximation for doped systems with small structural relaxations. For simplicity, we only compare the contributions from the zone-center phonon modes.

Because of the cubic symmetry, there are only four different optical phonon modes at Γ. We obtain their eigenvectors and frequencies by calculating the dynamical matrix corresponding to the zone-center phonons. For each frozen phonon mode j in the crystal, the self-consistent change in the crystal potential δV^j_Γ is computed. Then the electron-phonon matrix elements are obtained using $g^j_{nn'k} \equiv \langle nk|\delta V^j_\Gamma|n'k\rangle$. We find that the matrix elements between the same band are

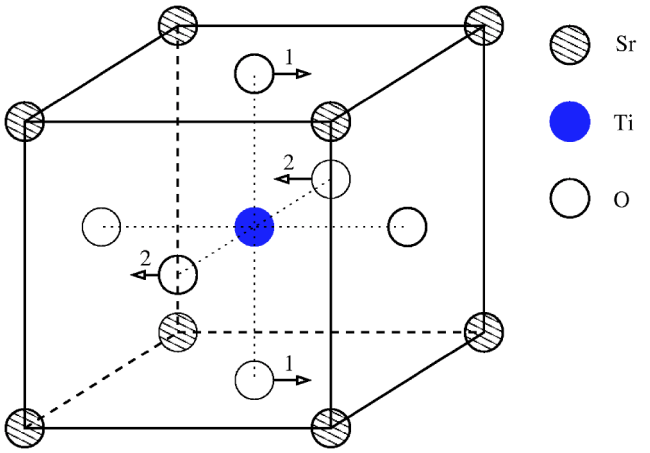

FIG. 7. The strongest-coupling zone-center phonon mode, involving only two of the oxygen atoms in the unit cell.

much larger than those between different bands. Also, for both the lowest conduction band and the highest valence band, one particular phonon mode involving only two of the oxygen atoms couples much stronger than all other Γ optical phonon modes, so only this phonon mode is used for our estimation. The polarization vector of this strongest coupling mode is shown in Fig. 7. The electron-phonon coupling in the highest valence band is much weaker than the lowest conduction band. For a typical k-point near the conduction band minimum at Γ, for example, at $k=(0.05,0.05,0.05)$ for the lowest conduction band, $|g_k^{nn}|^2/\hbar\omega \approx 2.25$ eV. While at $k=(0.45,0.45,0.45)$, which is near the valence band maximum at R, for the highest valence band $|g_k^{nn}|^2/\hbar\omega \approx 0.32$ eV. Since the density of states for the electron and hole doped systems are not too different, the difference of electron-phonon coupling strengths suggests that a superconducting transition in hole-doped systems will have a lower transition temperature than in electron-doped systems or none at all.

IV. SUMMARY

In the present work, we have investigated the structural and electronic properties of $SrTiO_3$ systems with both *n*-type and *p*-type doping using *ab initio* pseudopotential density functional theory. Structural relaxations due to doping are all small. Oxygen vacancies and substitution of V for Ti are considered for *n*-type doping. Oxygen vacancy doping induces Ti $3d$-e_g type defect states near the conduction band. The relative energy positioning depends on the local atomic relaxation and configuration. Some parts of the lower conduction bands become very flat in the case of electron doping by V substitution. For *p*-type doping, substitution of Sc for Ti is considered, and this produces a large density of states at the Fermi energy for comparable doping density. One particular phonon mode couples much stronger to both the conduction bands and the valence bands than other modes. Estimation of electron-phonon coupling strength indicates that a superconducting transition in hole-doped systems is less likely than for the electron-doped case despite the large density of states associated with the valence band states.

ACKNOWLEDGMENTS

This work was supported by National Science Foundation Grant No. DMR00-87088 and by the Director, Office of Science, Office of Basic Energy Sciences, Division of Materials Sciences and Engineering, U.S. Department of Energy under Contract No. DE-AC03-76SF00098. Computational resources have been provided by NSF at the National Partnership for Advanced Computational Infrastructure. One of the authors (W.D.) acknowledges the financial support from Ministry of Science and Technology of China, and the Berkeley Scholar Program.

[1] O. E. Kvyatkovskiĭ, Phys. Solid State **43**, 1401 (2001).
[2] K. A. Müller and H. Burkard, Phys. Rev. B **19**, 3593 (1979).
[3] W. Zhong and D. Vanderbilt, Phys. Rev. B **53**, 5047 (2000).
[4] Y. Aiura, H. Bando, I. Hase, Y. Nishihara, Y. Nishihara, Y. Haruyama, and H. Suzuki, Superlattices Microstruct. **21**, 321 (1997).
[5] N. Shanthi and D. D. Sarma, Phys. Rev. B **57**, 2153 (1998).
[6] T. Yokoya, T. Sato, H. Fujisawa, T. Takahashi, A. Chainani, and M. Onoda, Phys. Rev. B **59**, 1815 (1999).
[7] T. Jarlborg, Phys. Rev. B **61**, 9887 (2000).
[8] R. Astala and P. D. Britowe, Modell. Simul. Mater. Sci. Eng. **9**, 415 (2001).
[9] R. Astala and P. D. Britowe, J. Phys.: Condens. Matter **14**, L149 (2002).
[10] T. Higuchi, T. Tsukamoto, N. Sata, M. Ishigame, Y. Tezuka, and S. Shin, Phys. Rev. B **57**, 6978 (1998).
[11] T. Higuchi, T. Tsukamoto, K. Kobayashi, S. Yamaguchi, Y. Ishiwata, N. Sata, K. Hiramoto, M. Ishigame, and S. Shin, Phys. Rev. B **65**, 033201 (2002).
[12] K. van Benthem and C. Elsässer, J. Appl. Phys. **90**, 6156 (2001).
[13] R. D. King-Smith and D. Vanderbilt, Phys. Rev. B **49**, 5828 (1994).
[14] S. D. Mo, W. Y. Ching, M. F. Chisholm, and G. Duscher, Phys. Rev. B **60**, 2416 (1999).
[15] M. L. Cohen, Phys. Rev. **134**, A511 (1964).
[16] J. F. Schooley, W. R. Hosler, and M. L. Cohen, Phys. Rev. Lett. **12**, 474 (1964).
[17] C. S. Koonce, M. L. Cohen, J. F. Schooley, W. R. Hosler, and E. R. Pfeiffer, Phys. Rev. **163**, 380 (1967).
[18] N. E. Phillips, J. C. Ho, D. P. Woody, J. K. Hulm, and C. K. Jones, Phys. Lett. **29**, 356 (1969).
[19] N. E. Phillips, B. B. Triplett, R. D. Clear, H. E. Simon, J. K. Hulm, C. K. Jones, and R. Mazelsky, Physica (Amsterdam) **55**, 571 (1971).
[20] G. Binnig, A. Baratoff, H. E. Hoenig, and J. G. Bednorz, Phys. Rev. Lett. **45**, 1352 (1980).
[21] P. Hohenberg and W. Kohn, Phys. Rev. **136**, B864 (1964).
[22] W. Kohn and L. J. Sham, Phys. Rev. **140**, A1133 (1965).

[23] D. M. Ceperley and B. J. Alder, Phys. Rev. Lett. **45**, 566 (1980).
[24] J. Ihm, A. Zunger, and M. L. Cohen, J. Phys. C **12**, 4409 (1979).
[25] M. L. Cohen, Phys. Scr., T **T1**, 5 (1982).
[26] N. Troullier and J. L. Martins, Phys. Rev. B **43**, 1993 (1991).
[27] S. G. Louie, S. Froyen, and M. L. Cohen, Phys. Rev. B **26**, 1738 (1982).
[28] B. G. Pfrommer, M. Côté, S. G. Louie, and M. L. Cohen, J. Comput. Phys. **131**, 233 (1997).
[29] L. F. Mattheiss, Phys. Rev. B **6**, 4718 (1972).
[30] *Landolt-Börnstein LBIII/16a-Numerical Data and Functional Relation Relation in Science and Technology: Crystal and Solid State Physics*, edited by T. Mitsui and S. Nouma (Springer, Berlin, 1982).
[31] G. Fabricius, E. L. P. Blanca, C. O. Rodriguez, A. P. Ayala, P. de la Presa, and A. Lopez García, Phys. Rev. B **55**, 164 (1997).
[32] R. Astala and P. D. Britowe, Comput. Mater. Sci. **22**, 81 (2001).
[33] D. Ricci, G. Bano, G. Pacchioni, and F. Illas, Phys. Rev. B **68**, 224105 (2003).
[34] J. P. Buban, H. Iddir, and S. Ogut, Phys. Rev. B **69**, 180102(R) (2004).
[35] W. Gong, H. Yun, Y. B. Ning, J. E. Greedan, W. R. Datars, and C. V. Stager, J. Solid State Chem. **90**, 320 (1991).
[36] D. A. Muller, N. Nakagawa, A. Ohtomo, J. L. Grazul, and H. Y. Hwang, Nature (London) **430**, 657 (2004).